Journal of Asian Architecture and Building Engineering

ISSN: 1346-7581 (Print) 1347-2852 (Online) Journal homepage: www.tandfonline.com/journals/tabe20

Interaction Curve for High Performance Ferrocement in Biaxial State of Tension

P. Rathish Kumar & C.B.K Rao

To cite this article: P. Rathish Kumar & C.B.K Rao (2005) Interaction Curve for High Performance Ferrocement in Biaxial State of Tension, Journal of Asian Architecture and Building Engineering, 4:2, 475-481, DOI: 10.3130/jaabe.4.475

To link to this article: https://doi.org/10.3130/jaabe.4.475

Published online: 23 Oct 2018.

Interaction Curve for High Performance Ferrocement in Biaxial State of Tension

P. Rathish Kumar*[1] and C.B.K Rao[2]

[1] Lecturer, Civil Engineering Department, National Institute of Technology, Warangal, India
[2] Professor, Civil Engineering Department, National Institute of Technology, Warangal, India

Abstract

Ferrocement's attribute as a thin reinforced concrete and laminated cement based composite enables numerous applications where strong and tough protective shell is needed. It is used in the construction of cylindrical and spherical shells as liquid retaining structures. The stress condition at a point in such shell structures is biaxial state of tension-tension. A study on the behaviour of ferrocement in biaxial state is important for establishing a rational design. The authors carried out a full-fledged investigation on ferrocement under different biaxial stress conditions. The present investigation deals with the study of ferrocement in biaxial tension-tension based on hollow cylindrical specimens. An interaction curve is proposed to estimate the strength of ferrocement in biaxial tension-tension. The relationship between octahedral normal and shear stress is also presented.

Keywords: high performance ferrocement; biaxial; tension-tension; interaction curve; analytical model

Introduction

Ferrocement is a versatile composite construction material, consisting of small diameter wire meshes dispersed spatially in the mortar matrix (ACI committee 549, 1993, IFS Committee 10, 2001). It has an excellent property of mouldability into any structural form and shape. Being thin walled in nature, it is an ideally suitable material for construction of shell, folded plate structures etc. It has a great potential to be used for liquid retaining structures. An element isolated from such a type of structure, is a two dimensional element subjected to two in-plane normal stresses and one in-plane shear stress. As the applied loads are primarily carried through the development of membrane action, the behavior of ferrocement under in plane stresses needs to be established. The use of high performance mortar as the matrix for ferrocement improves strength and durability characteristics such as permeability and cracking of the composite (P. R.Kumar *et al*, 2002a, P.R.Kumar *et al*, 2002b, P. R.Kumar *et al*, 2004). The closer distribution and uniform dispersion of reinforcement transforms the brittle mortar into a distinctly different material from RCC (Naaman, 2000). The commonly adopted specimens for conducting tests in biaxial stress state are: cubes, solid cylinders, hollow cylinders and plates. In the present investigation, hollow cylindrical specimens were used to investigate the strength of high performance ferrocement in biaxial tension-tension (P. R. Kumar, 2003, P. R. Kumar 2004).

*Contact Author: Dr. P. Rathish Kumar
Department of Civil Engineering, National Institute of Technology, Warangal, Andhra Pradesh, India-506 004.
Tel: 0091-870-2462136 Fax: 0091-870-2459853
E-mail: rateeshp@yahoo.com
(Received October 19, 2004; accepted June 3, 2005)

Experimental Program

Hollow cylinders can be tested easily in all biaxial stress combinations. The test specimens were 200mm in height, 75mm in outer radius and 18mm in thickness. Slag cement, sand passing through JIS sieve No. 1.2 (1.18mm), optimum dosages of silica fume and a chemical admixture were used in the preparation of the high performance mortars. The mix proportion was cement to sand 1:1 with a water-cementitious ratio of 0.34. The silica fume was used as a partial replacement of 10% by weight of cement (P. R Kumar *et al* 2001). The use of silica fume increased the surface area of the mortar matrix enabling reduction in the workability. Water-reducing chemical admixture (superplasticizer) compensated the water demand (P. R. Kumar *et al* 2001). A number of 50mm diameter mortar cubes were cast with the same mortar as used for ferrocement hollow cylindrical specimens. The 28-day strength of the mortar was 60MPa. The properties of the wire mesh used are given in Table 1.

Table 1. Properties of Mesh Wire Used

Axial Direction of the Specimen	
Diameter of wire (mm)	0.47
Yield strength (MPa)	512.5
Ultimate strength (MPa)	525
Hoop Direction of the Specimen	
Diameter of wire (mm)	0.47
Yield strength (MPa)	510
Ultimate strength (MPa)	520

The variable in the investigation was specific surface factor (S_F) and was achieved by varying the number of layers of wire mesh. It was identified as an effective parameter influencing the mechanical properties of ferrocement in tension (C.B.K.Rao 1994) and compression (P.R.Kumar and G.R.Kumar 2002). The specific surface factor is given by the expression

$$S_F = s. \quad \sigma_y / \sigma_p \qquad (1)$$

where, s is the specific surface ratio. Specific surface ratio is the total surface area of contact of the reinforcement wires present in the direction of application of force in a given width and thickness of the specimen, to the volume of the mortar per unit length of the specimen, in the direction of loading with the same width and thickness. In the present case the total number of wires were 584, 730 and 876 respectively for four, five and six layers in the axial direction, while it was 583, 729 and 874 in the hoop direction. The specific surface ratio was hence calculated based on the number of wires in the perimeter and volume of the mortar and the values were found to be 1.066, 1.320 and 1.480 respectively for four, five and six layered specimens. If σ_y is the yield strength of the wires in the direction of force and σ_p is the plain mortar strength in compression, the specific surface factor can be calculated based on Eq-1. A total of 72 specimens were cast and tested, 36 for constant force in the horizontal direction and 36 for constant force in the vertical direction.

Preparation of specimen

The standard 150mm diameter and 300mm cast iron cylindrical mould was fitted with a 100mm high teak wood cylinder at the bottom. One more cylinder made of galvanized iron of a diameter equal to the inner diameter of the hollow cylindrical ferocement specimen and 100mm more in height than the specimen, was placed in the central recess of the bottom cylinder to obtain the required uniform thick annular space over a height of 200mm. A typical mould used for casting the specimens is shown in Fig.1.

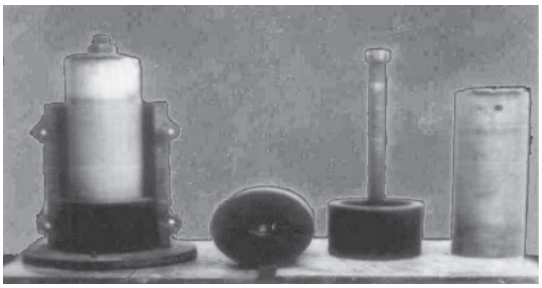

Fig.1. Mould Used

The required size of mesh was 195mm wide and of length slightly more than that required to obtain the number of layers, was cut from the standard mesh roll. The 195 mm long transverse wires formed the vertical axis of the specimen. The mesh was wound tightly to confirm with the cylindrical shape of the specimen. The fabricated mesh was placed in the annular space of the mould (Fig.2). Spacer rods were placed between the mesh layers and cover pieces were provided on the inner and outer surfaces. Mortar was filled in between the mesh layers, simultaneously vibrating the moulds. After about four hours of casting, the specimens were cured with damp burlap to prevent moisture loss. The specimens were stripped off the moulds 28 days after casting and then air cured before testing. Companion plain hollow cylindrical specimens were cast to obtain direct compression strength.

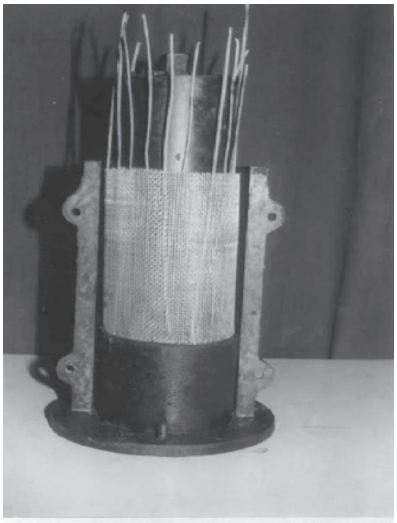

Fig.2. Fabricated Mesh and Spacer Rods

Test Set-up

The test setup for biaxial tension-tension consisted of an independent arrangement for applying tension in the hoop direction and vertical direction (Fig.3).

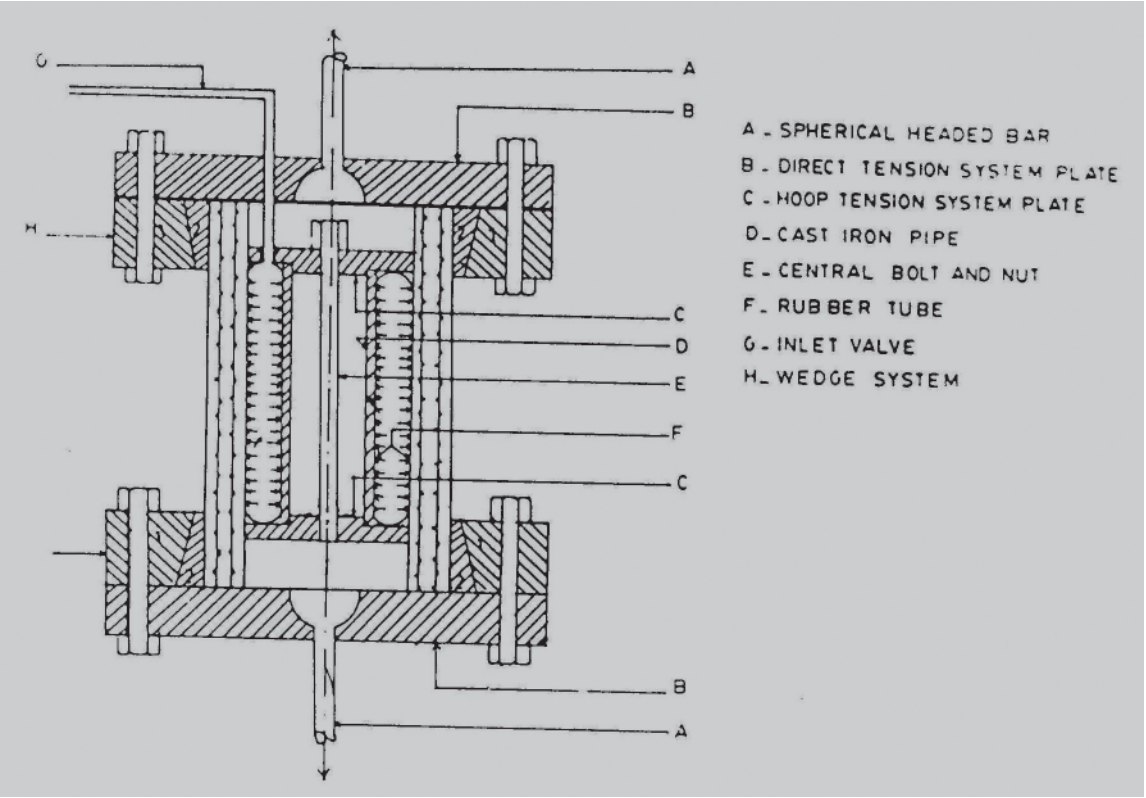

Fig.3. Schematic Diagram of the Test Setup

Specimens were subjected to circumferential tension by applying radial pressure by inserting a rubber tube in the annular space between the cast iron pipes and inflating the same by pumping oil through the inlet valve. The top and bottom steel plates restrain the expansion of the rubber tube, and thus the radial force was transferred to the inner surface of the ferrocement cylinder as a reaction. The tensile force in the vertical direction was applied using friction grips in the Universal Testing Machine of 100 Tonnes Capacity. Each system can be operated independently. Circular wedge friction grips were attached at the ends (Fig. 4a) and direct force was applied using a universal testing machine (Fig.4b).

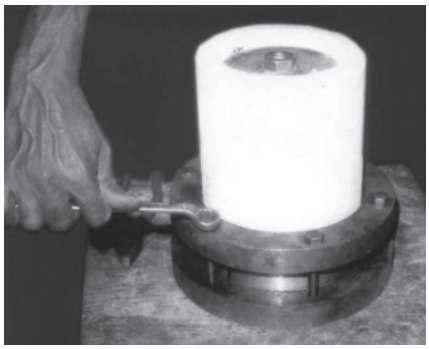

Fig.4 (a). Arrangement of the Wedge

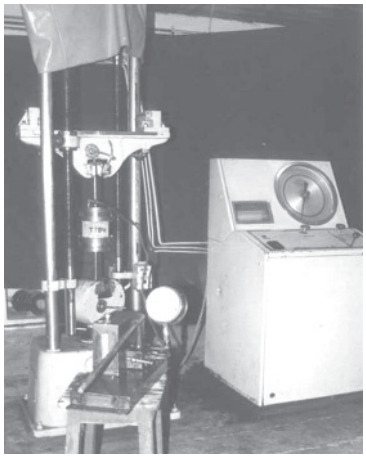

Fig.4 (b) A View of the Test Arrangement

Method of Testing

The general method of testing was to apply a constant force in one of the principal directions and increase the force in the orthogonal direction. Four discrete levels were taken in steps of 20% ranging from 20% to 80% of the theoretical axial and hoop tensile strength.

A predetermined force in one of the principal directions i.e. circumferential or axial was applied at a particular discrete level and maintained constantly. The force in the other principal direction was then increased gradually until failure occured. In the present investigation ferrocement specimens were tested by

both alternatives; method (a) with constant force in the horizontal direction; and method (b) with constant force in the vertical direction. It is known that the uniaxial tensile strength in the direction of force is equal to the load carrying capacity of the reinforcing wires in that direction (Naaman, 2000).

$$\sigma_t A_f = \sigma_{us} A_S \quad (2)$$

where, σ_t is the ultimate tensile strength of ferrocement, A_f is the cross sectional area of ferrocement, σ_{us} is the ultimate tensile strength of the reinforcing wires in the direction of the force and A_s is the area of reinforcing wires in the direction of force. The uniaxial strength of ferrocement in the principal directions i.e.; circumferential direction (σ_{th}) and axial direction (σ_{tv}) have been calculated from the above equation. It is known that the circumferential stress on the cross section of a thick cylinder subjected to internal pressure is non-uniform. However, the thin walled ferrocement specimens under investigation were treated as experiencing uniform stress such that the total force acting on the section was the same as that of non-uniform stress. Tensile stress in the circumferential direction satisfying the above assumption is given by the expression

$$\sigma_{th} = \frac{R_i}{R_o - R_i} P_i \quad (3)$$

where, P_i is the radial pressure and R_i is the internal radius and R_o is the outer radius of the cylinder. The uniaxial strength in the hoop/vertical direction is calculated using Eq. (2) and the radial pressure P_i to be applied is calculated using Eq. (3).

Behaviour under Load

Method (a) with constant force in the horizontal direction

The first crack was generally in the horizontal direction due to force in the vertical direction. Thereafter, the cracks formed at different sections and the number of cracks increased as the force increased. New cracks continued to form till the force in the vertical direction reached to about 90% of the peak value, while the earlier cracks widened and propagated in a direction inclined to the horizontal. The force in the vertical direction was nearly constant for a brief period on reaching a peak value. Attempts to increase the force further resulted in widening of the cracks. At this stage the reinforcing wires in the vertical direction snapped and the test was stopped after this peak value to avoid bursting of the tube. It was noticed that the force in the vertical direction at the first crack stage in biaxial tension was generally equal to the load carrying capacity of the reinforcing wires in uniaxial tension in that direction. The cracks were interconnected and were around the surface (Fig.5). As the steel content increased, more cracks of a smaller width were observed. Cracks similar to the outer ones were observed at the inner surface also.

Method (b) with constant force in the vertical direction

A predetermined force in the vertical direction was applied and maintained constantly while the force in the horizontal direction was increased later. The first cracks were observed in the vertical direction. The number of cracks increased with an increase in the fluid pressure. New cracks were formed until the fluid pressure reached 90% of the peak value, while the cracks formed earlier widened and propagated in the same direction (Fig.6).

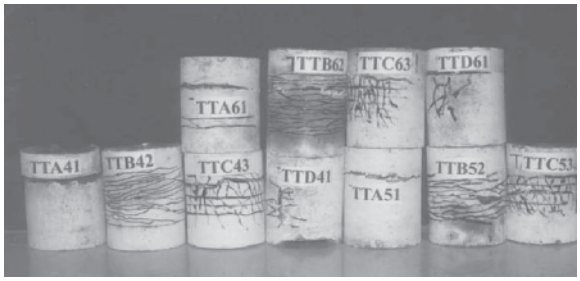

Fig.5. Crack Pattern for Specimens (Method a)

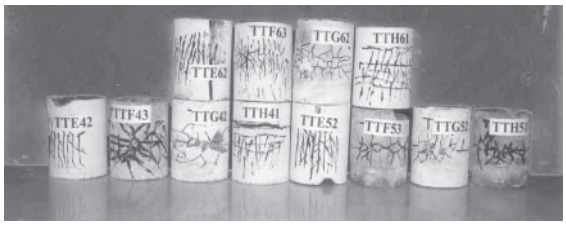

Fig.6. Crack Pattern for Specimens (Method b)

Attempts to increase the fluid pressure, on its reaching a peak value, resulted in a momentary increase; but returned to the previous level, further widening the cracks. Attempts to snap the wires in the horizontal direction resulted in bulging of the specimen between the wedge grips. The test was stopped at this stage. It was observed that the tensile stress in the horizontal direction at the first crack stage in the biaxial condition was the same as uniaxial ultimate tensile strength in that direction. The number of cracks increased with an increase in the steel content. Cracks similar to those at the outer surface were observed at the inner surface also. It was noted that the behaviour of ferrocement specimens was similar in biaxial tension-tension to that in the alternate methods of testing.

Interaction Diagram

The uniaxial ultimate strength in the vertical direction (σ_{tv}) and the horizontal direction (σ_{th}) of a typical four-layered ferrocement specimen is given in columns four and five of Table 2. For the values noted at the peak stage during test under the biaxial state, the tensile strength in the horizontal direction (σ'_{th}) is

calculated using Eq. (3) and the strength in the vertical direction (σ'_{tv}) is calculated conventionally. The values are reported in columns six and seven of the table respectively. The prefixes A, B, C and D indicate the discrete levels of 20%, 40%, 60% and 80% of the ultimate tension in the hoop direction, while E, F, G and H are the discrete levels for the same percentage of maximum tension in the axial direction. 41, 42 and 43 indicate the number of the four-layered specimens for that discrete level respectively. Similar results were obtained for five and six layered ferrocement specimens also.

An examination of the values obtained shows that the tensile strength in the direction orthogonal to the direction of application of predetermined constant force is always greater than the uniaxial tensile strength in that direction owing to the Poisson's effect. It increased initially and decreased later. This was found to be true

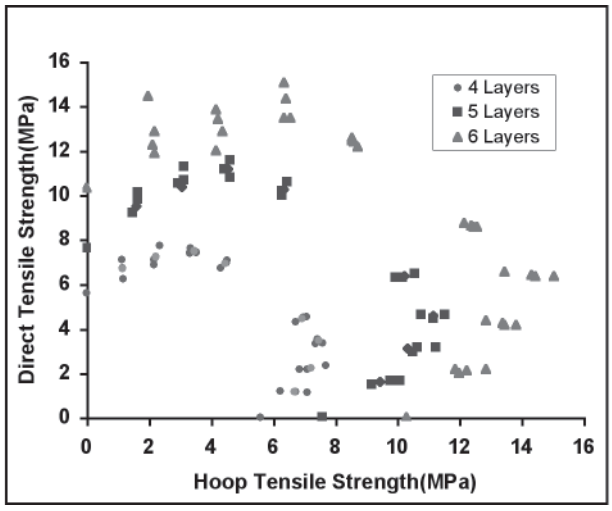

Fig.7. Interaction Diagram

Table 2. Strength of Ferrocement Specimens under Biaxial Tension-Tension

S.No	Specimen Desg.	Plain Mortar Strength(MPa)	Analytical Uniaxial Tensile Strength (MPa)		Experimental Biaxial Tensile Strength (MPa)		Non-Dimensionalised Strength values	
			σ_{tv}	σ_{th}	σ'_{tv}	σ'_{th}	$\sigma'_{tv} / \sigma_{tv}$	$\sigma'_{th} / \sigma_{th}$
(1)	(2)	(3)	(4)	(5)	(6)	(7)	(8)	(9)
1	TTA41	58.5	5.59	5.62	6.73	1.16	1.2	0.21
2	TTA42				7.1	1.14	1.27	0.2
3	TTA43				6.24	1.17	1.12	0.21
4	TTB41				6.86	2.16	1.23	0.38
5	TTB42				7.71	2.35	1.38	0.42
6	TTB43				7.1	2.16	1.27	0.38
7	TTC41				7.1	2.16	1.27	0.38
8	TTC42				7.43	3.53	1.33	0.63
9	TTC43				7.6	3.34	1.36	0.59
10	TTD41				6.97	4.51	1.24	0.8
11	TTD42				6.74	4.31	1.2	0.77
12	TTD43				7.08	4.53	1.26	0.81
13	TTE41	56.5	5.59	5.62	1.1	6.99	0.2	1.24
14	TTE42				1.1	7.87	0.2	1.4
15	TTE43				1.1	6.39	0.2	1.14
16	TTF41				2.17	6.96	0.39	1.24
17	TTF42				2.17	7.85	0.39	1.4
18	TTF43				2.17	7.12	0.39	1.27
19	TTG41				3.32	7.35	0.59	1.31
20	TTG42				3.32	8.31	0.59	1.48
21	TTG43				3.32	8.12	0.59	1.44
22	TTH41				4.34	6.9	0.78	1.23
23	TTH42				4.44	7.19	0.79	1.28
24	TTH43				4.47	7.57	0.8	1.35

in the case of five and six layered specimens also. The trend was the same irrespective of the specific surface factor and the method of testing viz., method (a) and (b). The trend is depicted in Fig.7.

To normalize the effect of specific surface factor, tensile strength in the biaxial states of each direction are divided by the uniaxial ultimate strength in their respective directions. The superposed normalized interaction diagrams $\sigma'_{tv} / \sigma_{tv}$ vs. $\sigma'_{th} / \sigma_{th}$ of four, five and six layers are shown in Fig.8.

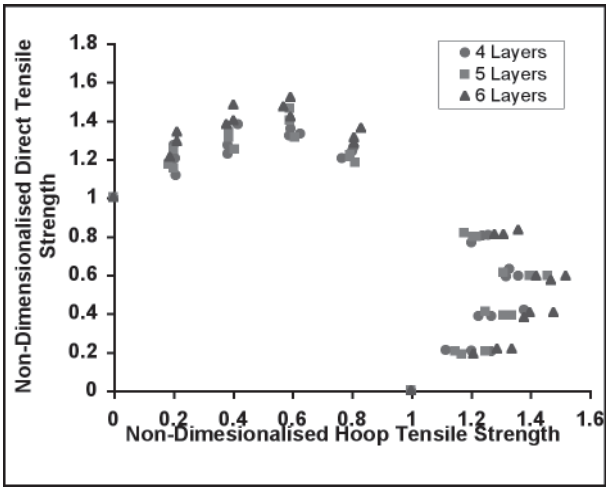

Fig.8. Normalized Interaction Diagram

It can be seen from Fig.8 that after normalization there is no influence of specific surface factor or steel content on the interaction diagram. The trend of the interaction diagram is the same in either method of testing, meaning that the behaviour of ferrocement specimens in biaxial tension-tension is symmetrical about a 45º line. Method (b) gave slightly higher values of $\sigma'_{th} / \sigma_{th}$ than its symmetrical value of $\sigma'_{tv} / \sigma_{tv}$ in method (a). This difference may be due to the effect of the wedge grips, which might have induced additional restraint on the edges of the specimen as evidenced by bulging in the central portion of the specimen. The assumptions of symmetry of behaviour about a 45º line, provides a conservative and safe condition.

Analytical Model

The normalized interaction diagram is not influenced by the steel content vide Fig.8., further, there seems to be a definite trend between the direct non-dimensionalised and hoop tensile strengths. A best fit between these points, seemed to follow the path of part of a parabola. An equation of the form $y = a + bx + cx^2$ was fitted for one half the symmetrical part of the interaction diagram and the constant values were obtained. The regression equation obtained is

$$\frac{\sigma'_{tv}}{\sigma_{tv}} = 1.0 + 1.3678\frac{\sigma'_{th}}{\sigma_{th}} - 1.2749\left(\frac{\sigma'_{th}}{\sigma_{th}}\right)^2 \qquad (4)$$

The path of the above equation is plotted as shown in Fig.9. The correlation coefficient was 0.98. The other half of the interaction diagram was also similar to the first symmetrical half.

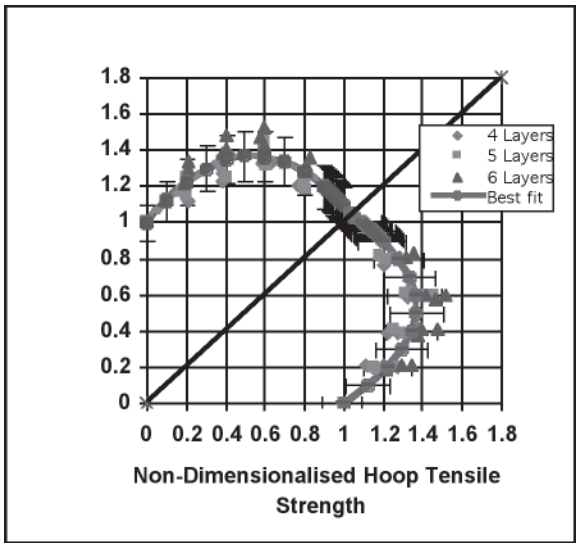

Fig.9. Normalized Interaction Curve

The equation can hence be used to predict the behaviour of ferrocement in biaxial tension-tension. The 10% error bars for x and y directions were plotted and it was noted from the diagrams that all the experimental points were well within the 10% range.

Failure criteria for tension-tension

Nadai's concept of octahedral shear stress, which is a function of octahedral normal stress as a failure criterion was investigated, as it seemed applicable to ferrocement. Applying Nadai's theory to ferrocement the octahedral normal stress (σ_o) and octahedral shear stress (τ_o) were computed for the test data using formulae

$$\sigma_o = \frac{\sigma_1 + \sigma_2 + \sigma_3}{3} \qquad (5)$$

$$\tau_o = \frac{1}{3}\sqrt{(\sigma_1 - \sigma_2)^2 + (\sigma_2 - \sigma_3)^2 + (\sigma_3 - \sigma_1)^2} \qquad (6)$$

where, σ_1, σ_2, σ_3 are principal stresses. σ_3 is zero as the problem is a plane stress problem. The values of so and to are given in Table 3. for biaxial tension-tension. TX4, TX5 and TX6 in the table indicate uniaxial specimens. The plot of σ_o vs. τ_o is shown in Fig.10. There is a good correlation between σ_o and τ_o.

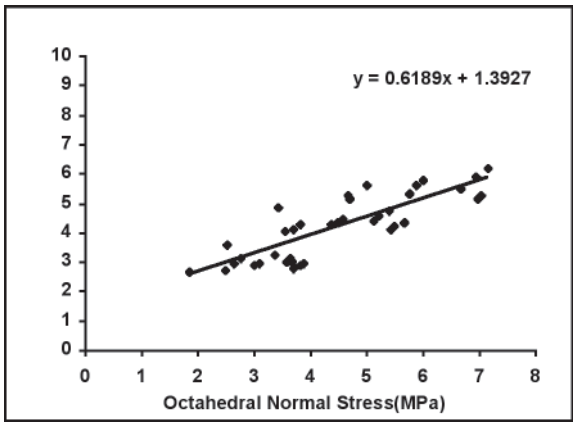

Fig.10 Octahedral Shear Stress vs Normal Stress

Table 3. Octahedral Normal and Shear Stresses of Ferrocement Specimens in Biaxial Tension-Tension

Desg.	Octahedral Normal Stress σ_o (MPa)	Octahedral Shear Stress τ_o (MPa)	Desg.	Octahedral Normal Stress σ_o (MPa	Octahedral Shear Stress τ_o (MPa)	Desg.	Octahedral Normal Stress σ_o (MPa	Octahedral Shear Stress τ_o (MPa)
TX4	1.86	2.64	TX5	2.53	3.58	TX6	3.43	4.86
TTA41	2.63	2.94	TTA51	3.55	4.02	TTA61	5.01	5.62
TTA42	2.75	3.11	TTA52	3.69	4.1	TTA62	4.69	5.16
TTA43	2.47	2.71	TTA53	3.82	4.28	TTA63	4.66	5.25
TTB41	3.01	2.86	TTB51	4.37	4.27	TTB61	6.00	5.80
TTB42	3.35	3.23	TTB52	4.49	4.32	TTB62	5.74	5.34
TTB43	3.09	2.97	TTB53	4.56	4.42	TTB63	5.88	5.63
TTC41	3.57	3.02	TTC51	5.20	4.59	TTC61	6.68	5.5
TTC42	3.65	3.03	TTC52	5.39	4.74	TTC62	7.14	6.17
TTC43	3.65	3.11	TTC53	5.13	4.42	TTC63	6.93	5.91
TTD41	3.83	2.89	TTD51	5.49	4.19	TTD61	7.04	5.24
TTD42	3.68	2.79	TTD52	5.41	4.11	TTD62	6.96	5.12
TTD43	3.87	2.93	TTD53	5.68	4.35	TTD63	7.00	5.20

The relationship between octahedral normal and shear stress for biaxial stress state in tension-tension can hence be expressed as

$$\tau_o = 1.3927 + 0.6189\sigma_0 \qquad (7)$$

Conclusions

The test setup designed was suitable for testing hollow cylindrical specimens in biaxial tension-tension. Some of the important conclusions obtained from the experimental investigation are:

1) Stress in one direction was found to be beneficial to strength in the orthogonal direction as observed from the normalized interaction diagram.

2) The trend of the interaction diagram was not affected by the specific surface factor (S_F), whereas the individual values of strength were dependent on S_F.

3) An interaction curve and hence a mathematical model was developed for the high performance ferrocement which can be used as a criterion for design of ferrocement surfaces under biaxial tension-tension.

4) From the crack pattern it may be concluded that there is adequate ductility in ferrocement as these specimens continued to resist load even after the total propagation of cracks in the thickness of the specimen.

5) Nadai's concept of octahedral shear stress being a function of octahedral normal stress is found to be applicable to ferrocement. A relationship between octahedral normal and shear stress for high performance ferrocement is suggested.

6) High performance ferrocement is ideal for use in stressed skin surfaces owing to its superior performance in strength, ductility and crack resistance.

Acknowledgements

The authors gratefully acknowledge the financial support provided by the Director, National Institute of Technology, Warangal, India for the carrying out of this research work.

References

1) ACI Committee 549 (ACI 549. 1R-93, 1993) Guide for Design, Construction and Repair of Ferrocement, American Concrete Institute, 1-10.
2) IFS Committee 10 (2001), Ferrocement Model Code, Building Code Recommendations for Ferrocement, 1-2.
3) Naaman A.E (2000), Ferrocement and Laminated Cementitious Composites, Techno Press-3000, 1st Edition.
4) P.R.Kumar, D.R.Seshu, M.Sudhakar (2001), Effect of water-cementitious ratio on the compressive strength of silica fume concrete, Journal of Indian Concrete Institute, Vol. 2, 24-28.
5) P.R Kumar (2001) , Superplasticizers in High Strength Mortars for use on Ferrocement Works 26th International Conference on Our World in Concrete and Structures organized by CI-Premier Pte Ltd at Singapore.
6) P.R.Kumar, G.R.Kumar (2001), Ferrocement-An effective way of confining high strength concrete, Journal of Bridges and Structural Engineering, IABSE, Vol. 32, No. 3, September 2002.
7) P.R Kumar, Seshu D.R and Rao C.B.K (2002 a), Some Studies on High Performance Mortar Mixes (Part-1 Strength and Flow Characteristics, Journal of Ferrocement, AIT Thailand, Vol. 32, No. 3, 205-214.
8) P.R Kumar, Seshu D.R and Rao C.B.K (2002 b), Some Studies on High Performance Mortar Mixes (Part-2 Shrinkage and Sorptivity Characteristics, Journal of Ferrocement, AIT Thailand, Vol. 32, No.3, 215-231.
9) P.R Kumar (2003), Ferrocement with High Performance Mortar in Biaxial States of Stress, Doctoral thesis submitted to the National Institution of Technology, Warangal, India.
10) P.R.Kumar, Toshiyuki Oshima, Shuichi Mikami, Tomoyuki Yamazaki (2004), Improvement in strength and ductility of reinforced concrete columns with ferrocement jacketing, Proceedings of the International Workshop on Modern Science and Technology, Organized by Kitami Institute of Technology, Japan, 302-307.
11) P.R. Kumar, Toshiyuki Oshima, Shuichi Mikami, Rao C.B.K (2004), High Performance Ferrocement (HPF) under Axial Compression, Proceedings of the Sixth International Summer Symposium Organized by Japan Society of Civil Engineers (JSCE), Saitama, Japan, ISSN: 1345-8507, 29-32.
12) Rao C.B.K and Rao A.K (1994), Stress-Strain relationship for Ferrocement in Tension, Journal of Ferrocement, Vol. 24, No. 4, October 1994, PP 309-320.